The Journal of

Imaging Science
and Technology

△ **IS&T**

The Society for Imaging Science and Technology
http://www.imaging.org

Perceptual Representation of Textured Images

Xavier Otazu and Maria Vanrell▲
Computer Vision Center, Dept. Informàtica (UAB), Edifici O, Campus UAB, Barcelona, SPAIN

Chromatic induction effects depend, among others, on the frequency content of the observed region. Highly textured images usually show some dominant frequency information, which produces prominent chromatic induction effects when observed. As it is shown by some authors, the two chromatic induction effects, i.e., chromatic contrast and assimilation, can be computationally simulated by blurring and sharpening operators, respectively. In this article, we present a first approximation to the perceptual representation of highly textured images using a wavelet decomposition approach. Wavelet coefficients are modulated by a weighting function, which performs either assimilation or contrast at every frequency level of the image. This wavelet approach allows us to define both chromatic induction effects in a unified framework as a single mathematical operator.

Introduction

Modeling low level vision processes is one aim of computer vision research. The goal of this research is to build a visual front-end,[1] that is a computational representation of the image that provides us with the appearance information of the image content. Appearance depends on the observation distance, as well as considerations on the physiological attributes of the human visual system, since acquisition devices does not act exactly as the human visual system does. In this article we deal with the goal of building perceptual images. We will focus on two aspects: color and spatial frequency. There is some work dealing with these two aspects.[2–5] The novelty of this work relies on the use of a unified mathematical model to represent two common induction phenomena.

The representation of the appearance of color and spatial frequency is relevant to many industrial applications where color texture images are involved. Several production processes require the measurement of color of non-homogeneous surfaces, such as tile, steel, textiles, printed paper or wood. In these cases, color cannot be measured using common colorimetric devices, since the integration of textured surfaces does not provide useful measurements of the color appearance; a perceptual representation of the digital color image is required in order to give the basis for further processing based on this perceived color.

In color literature the changes in perceived color caused by surrounding stimuli are referred as color induction mechanisms.[6] Smith et al.[7] measured the relationship between spatial frequency and color induction effects, concretely on assimilation and contrast induction mechanisms.

In this work we propose a mathematical model to unify these two phenomena in order to represent their appearance. To this end, the article has been organized as follows: first we give basic definitions about color induction and its relationship with the perception of textures; second, we give a brief overview of the wavelet analysis; afterward and based on this mathematical model, we propose a unified approach to represent color induction effects; finally we discuss the results on how the model acts on some examples and present some conclusions and further research directions.

Color Induction

Land et al.[8] showed how the color perceived by the human visual system of a surface does not match with the physical light emitted by this surface. In this case, the perceptual representation of the color of a point depends on something more than just the physical properties of that point. There are simple and well known examples that easily show how color appearance or perceived color can change depending on the image content.[9]

In color science, color induction refers to the change in perceived color of a light source caused by a nearby inducing stimulus.[8,10] Land et al.[8] demonstrated how a test color appearance changes depending on its surround. An example is shown in Fig. 1. On the right half of the image, a color contrast effect makes the blue bands seems more blue and the yellow bands more yellow. However, on the left half of the image an assimilation process induces color appearance tends to be greenish.

These induction effects can be generically explained in terms of local spatial frequency of the image as has been shown by Smith.[7] In the first case, the low frequency prop-
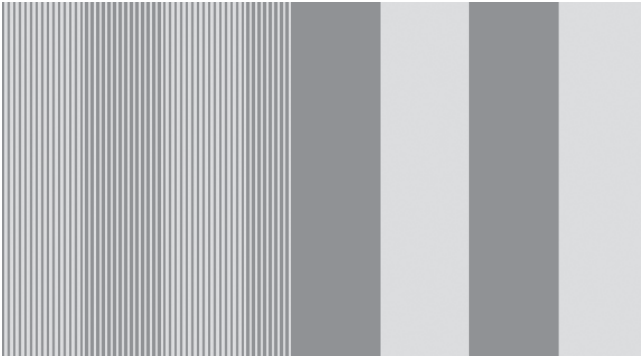
Figure 1. Synthetic image containing yellow and blue gratings of different spatial frequency. *Supplemental Material— Figure 1 can be found in color on the IS&T website (www.imaging.org) for a period of no less than two years from the date of publication.*

erty of the image test induces a chromatic contrast effect, that is, perceived chromaticity moves away from its direct surround, which could be computationally interpreted as the application of a sharpening operator. Meanwhile, in the second case, the high frequencies of the image patterns induce an assimilation effect, that is, chromaticity moves toward the chromaticity of its direct surround, which can be computationally represented by convolving the image with a blurring operator.

Textures
Texture images are those images presenting certain basic elements, textons, which are repeated all over the image forming global emergent patterns that can be random or regular. They usually present a specific global spatial frequency property. These basic texton elements can be of different colors, and the perception of this color is influenced by this spatial frequency properties.

Color texture images are usually used in manufacturing processes. Measurements of color on textured images can be used to classify the production, to calibrate the production process parameters, to perform color measurements or just to do quality control. Texture analysis and segmentation of its basic elements is needed to deal with reliable color measurements, and they has to agree with the judgments provided by human observers, therefore, an appearance representation of this color texture images is required.

In this work we propose a model to build a tower of images for a given image. Chromaticity properties of these images have been modified considering two factors: the appearance from different observation distances, and the spatial frequency of the image content. The changes are done in accord with the induction mechanisms of the human visual system we have introduced previously. This set of images is the basis for further progress towards achieving an appearance based analysis of these texture images.

Wavelets
Multiresolution analysis based on wavelet theory introduces the concept of details between successive levels of scale or resolution.[11–13] Wavelet decomposition is widely used in Image Processing and it is based on the decomposition of the data set into multiple channels according to their local frequency content. Wavelet transform decomposes data sets into a number of new sets, each one with distinct frequency information.

Given an image, I, its wavelet decomposition is denoted by:

$$WT(f) \equiv \omega_{j,n}(I) = \left\langle I \middle| \psi_{j,n} \right\rangle = \int_{-\infty}^{\infty} I(Z)\psi_{j,n}^*(z)dz \quad (1)$$

where $\psi_{j,n}^*$ are the conjugate wavelet basis functions with parameters, j and n, related to the scale and pixel position respectively, and $\omega_{j,n}(I)$ is the decomposition coefficient of image I of pixel n and for the j wavelet plane. Given this decomposition, the original image can be completely recovered by integrating the coefficients with the basis functions. Although this is the general approach, in this work we will work on a particular case, it is the *à trous* algorithm.[14] In this algorithm, a sequence of images c_i is obtained by iteratively convolving these images by a low pass filter h. The difference between two consecutive images is the ω_j wavelet plane associated to a certain resolution j. This compact ω_j notation for the wavelet coefficients refers to the set of all the coefficients n, at a certain resolution j. Using a one-dimensional notation for the sake of simplicity, we can see an initial discrete signal $c_0(k)$ (in the present case it would be an image, $I \equiv c_0(k)$) as a projection of continuous function $f(t)$ on a discrete V_0 space spanned by $\phi(t)$ basis functions, called scaling functions. The projection on a subspace $V_j \subset V_0$,

$$c_j = \left\langle f(t) \middle| \frac{1}{2^j} \phi\left(\frac{1}{2^j} - k\right) \right\rangle \quad (2)$$

is then an approximation of c_0 at scale or resolution j. The approximation of coefficients c_{j+1} at scale $j + 1$ can be calculated by means of the discrete convolution of coefficients c_j at scale j with a filter h,

$$c_{j+1}(k) = h(n) * c_j(k + n2^j), \quad (3)$$

and the wavelet coefficients can be calculated as the difference between two consecutive scales,

$$\omega_j(k) = c_{j-1}(k) - c_j(k). \quad (4)$$

This expression can be developed to show its recursive nature as a function of the original image I and the filters h_i:

$$\omega_0 = (I * h_0) - I \quad (5)$$

$$\omega_1 = ((I * h_0) * h_1) - (I * h_0) \quad (6)$$

$$\vdots \quad (7)$$

$$\omega_j = (\cdots((I * h_0) * h_1) * \cdots * h_j) - (\cdots(I * h_0) * \cdots * h_{j-1}) \quad (8)$$

In our case we have used a B_3 spline function for the scaling function $\phi(t)$, which leads to a $h(n)$ function that can be approximated by a Gaussian kernel. The h_i filters are resampled versions of the original $h(n)$ kernel. It is performed in order to accommodate, into the above convolution of this kernel with the original I image, the convolution of this kernel on the resampled $c_j(k + n2^j)$ data in Eq. (3).

The reconstruction of the original signal is simply the sum of all the wavelet coefficients plus the residual approximation $c_N(k)$,
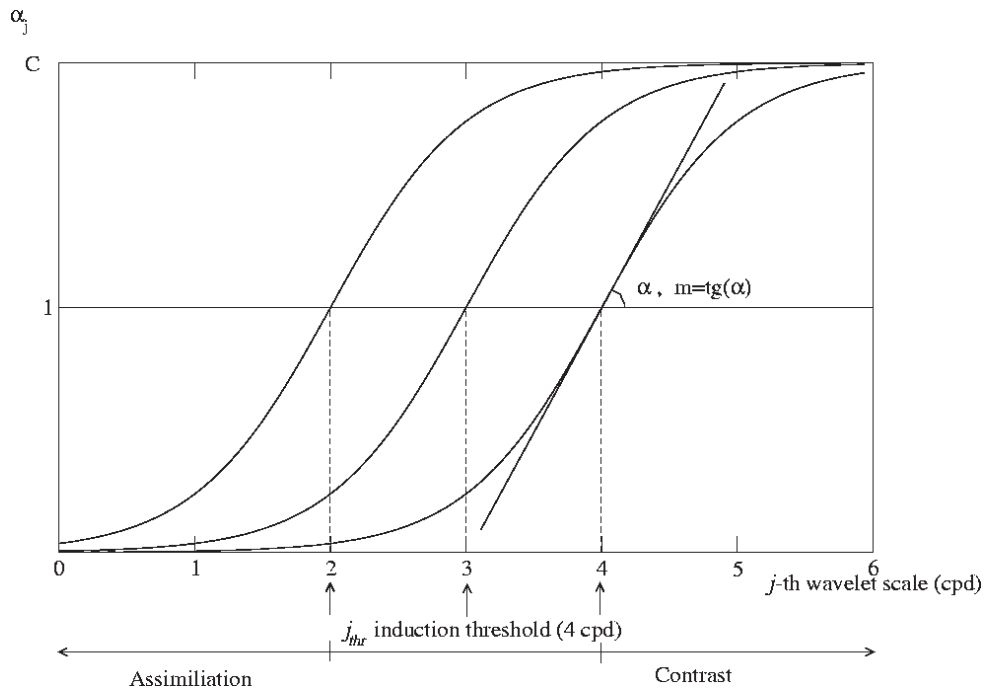
Figure 2. Parameter α_j displayed as a function of wavelet scale j.

$$I \equiv c_0(k) = \sum_{j=1}^{N} \omega_j(k) + c_N(k), \qquad (9)$$

where N is the number of resolutions, usually called wavelet planes, into which the original signal is decomposed. Every wavelet plane $\omega_{j,n}(I)$ can be related to features of a certain frequency $v(j)$.

From a computer vision point of view, the *à trous* algorithm can be understood as a multi-scale Laplacian filtering,[15] where high frequency edges are separated on low index coefficients and low frequency edges appear on high index coefficients.

Perceptual Wavelet Model

Computational modeling of chromatic induction effects can be given by several image processing operators. Particularly, assimilation effects can be simulated by an image blurring process.[2] The practical effect of a blurring process is that it reduces differences between neighbor points, hence, a smoother image is obtained. On the other hand, computational implementations of chromatic contrast can be simulated by an image sharpening process,[3] which enhances differences between neighbor points.

These computational approximations are performed independently, that is, they are described as different processes and implemented using different filters. Specifically, a blurring effect can be implemented using a low pass filter, whereas a sharpening effect can be implemented using a high pass filter. In this work, we present a wavelet based chromatic induction model, which allows to describe these two chromatic induction effects in a single mathematical expression. In this model, chromatic assimilation and chromatic contrast are simultaneously performed depending on the frequency content of the textured image.

Blurring and sharpening processes can be implemented in wavelet space modifying the values of wavelet coefficients. In particular, a blurring effect can be approximated by reducing the value of some frequency wavelet coefficients, mainly those related to the higher frequencies. On the other hand, a sharpening effect can be approximated by enhancing some wavelet coefficients. We can perform these blurring and sharpening processes introducing a weighting parameter α_j into the wavelet decomposition of our image I,

$$I(k,l) = \sum_{j=0}^{N} \alpha_j \cdot \omega_j(k,l) + c_N(k,l), \qquad (10)$$

where (k,l) is the image coordinates of a pixel in the k-th row and l-th column, and N the number of wavelet planes into which the image is decomposed.

Parameter α_j defines the specific process, i.e., blurring or sharpening, to apply on the coefficients of the j-th wavelet plane. When $\alpha_j < 1$ differences between wavelet coefficients are reduced, thus a blurring process is performed. When $\alpha_j > 1$, differences are enhanced, thus a sharpening process is performed. Hence, the model performs a blurring process on some wavelet planes and a sharpening process on others, producing a final image which shows both effects.

As explained above, and shown in several studies,[2,7,8] for higher frequency features (lower j values) we have to perform assimilation, i.e., $\alpha_j < 1$ and for lower frequencies (higher j values) we have to perform chromatic contrast, i.e., $\alpha_j > 1$. It suggests that parameter α_j should be an increasing function in j. As a first approximation, a possible generic profile for the α_i function is shown in Fig. 2. Several mathematical expressions could be used for this α_j function, such as truncated Gaussians, sigmoids, etc., but a correct evaluation of this function should be obtained from psychophysical experiments. Several psychophysical works[7,16,17] show that the degree of chromatic contrast presents a bound on its maximum value. That is, there exists a maximum value $\alpha_j \equiv C > 1$

Otazu and Vanrell

for the enhancement factor to perform chromatic contrast on image features. If α_j function had to mimic this behavior, it should present some asymptotic behavior towards this maximum C of contrast factor. A value of $C = 3/2$ value has been suggested for region contrast enhancement.[2,9]

Since the function α_j presents a maximum at $C > 1$, we can define a j_{thr} threshold value, where $\alpha_{thr} \approx 1$, that defines the frequency at which neither chromatic assimilation nor chromatic contrast is performed. This j_{thr} threshold value defines the frequency which separates the chromatic assimilation and chromatic contrast effects, that has been established as around 4 cpd (cycles per degree).[7]

Taking into account all these properties, and as a first approximation, the α_j function can be modeled as

$$\alpha_j = \frac{C}{1 + \exp\{m \cdot (j_{thr} - j)\}}, \qquad (11)$$

where C defines the maximum enhancement factor applied to image features when performing chromatic contrast, j_{thr} parameter is the induction threshold, and the factor m defines the slope of the α_j function around the central j_{thr} coordinate.

Since the j_{thr} induction threshold value is defined in visual angle unities, it can also be defined by a distance x_{thr} variable. Given an observation distance, the induction threshold, which is an angle, can be projected on the image spatial coordinates. That is, given a feature that present a visual angle β when observed at distance d the feature size s is

$$s = d \cdot \tan \beta. \qquad (12)$$

This projection is measured on the image space as a spatial measure, which in turn can be related to a period, i.e., a cycle, of spatial frequency. By definition, a wavelet scale j is related to a certain frequency $v(j)$. i.e., to a period

$$T = \frac{1}{v(j)}.$$

This relation is defined by

$$2^j = T = \frac{s}{s_p},$$

where

$$\frac{s}{s_p}$$

is the number of pixels in one frequency.period T, and s_p is the image pixel size. Since the induction threshold value is defined as including 4 cpd in this wavelet space, we can define

$$4T = 2^{j_{thr}} = 4\frac{s}{s_p} \qquad (13)$$

The term j_{thr} is the image wavelet scale associated to the projection of 4 cpd when observing the image from distance d.

Therefore, inserting Eq. (12) into Eq. (13), we finally obtain

$$j_{thr} = \log_2\left(\frac{4d\tan 1°}{s_p}\right). \qquad (14)$$

The j_{thr} factor is the wavelet scale associated to the $v(j_{thr}) = 4$ cpd induction threshold value when observing an image with a pixel size sp from a distance d. Variation of the distance at which the image is observed is defined as a translation of the α_j function along the j coordinate. To move away from the image is equivalent to shifting α_j towards lower frequencies (higher i values), since assimilation is produced only on the highest image frequencies. This translation is performed by the j_{thr} term.

Thus far, we have defined C and j_{thr} terms but no attention has been paid to m. The m term defines the function slope around the central j_{thr} induction threshold value. As stated in Ref. [7], at a frequency of 2 cpd the degree of chromatic contrast effect does not increase. This implies that 2 cpd $\equiv 2^{-1}$ ξ $v(j_{thr})$. On the other hand, it is around 9 cpd where the influence of chromatic assimilation reaches a maximum value, i.e., at an approximate frequency 2 • $v(j_{thr})$. In wavelet notation 2^{-1} ξ $v(j_{thr})$ $\equiv v(j_{thr} - 1)$ and 2 • $v(j_{thr}) = v(j_{thr} + 1)$, which means that wavelet planes prior to and subsequent to the j_{thr} plane are close to the saturation values. It suggests $m \approx 2$, and simple empirical experiments show that $m \approx 2.5$ is a good approximation value.

Finally, we can define a wavelet based model to implement chromatic induction effects. Using Eqs. (14), (10) and (11), we obtain

$$I(k,l) =$$
$$\sum_{i=0}^{N} \frac{C}{1 + \exp\left\{m \cdot \left(\log_2\left(\frac{4 \cdot d \cdot \tan 1°}{s_p}\right) - i\right)\right\}} \cdot \omega_i(k,l) + c_N(k,l) \qquad (15)$$

This expression simultaneously performs assimilation and chromatic contrast depending on both the local information of the image and the observation distance. In this model, distance d and pixel size s_p are the only free values that have to be defined *a priori*.

This induction model has been applied on the opponent color space, since this space has been shown[4,18,19] to be one of the best suited to the human visual system. Equation (15) has been applied to every channel of the opponent color space. An open issue is whether all opponent channels behave equally in front of similar stimulus. As stated in these references each chromatic channel does not present the same behavior in response to a particular spatial frequency; thus a different process has to be adopted for every opponent color channel. This suggests that different α_j functions have to be defined for every opponent channel. However, and as a first approximation, in this work all opponent color channels are treated equally.

Neighborhood integration and remote enhancement concepts have been proposed by several authors.[2,3,11] Each of these models takes into account the effect of close and distant regions to perform assimilation and contrast effects, but these effects are described separately, as independent effects and in a non-unified way. In the wavelet model we propose, all these effects are unified and described in a single α_j function, which explicitly states that assimilation and chromatic contrast effects can be seen as different interpretations of a unique and single process.

A similar multiscale model has been proposed,[20,21] called the ODOG model. The ODOG model also uses center-surround information at different frequencies, but it is formulated using anisotropic DOG (Difference

(a)

(b)
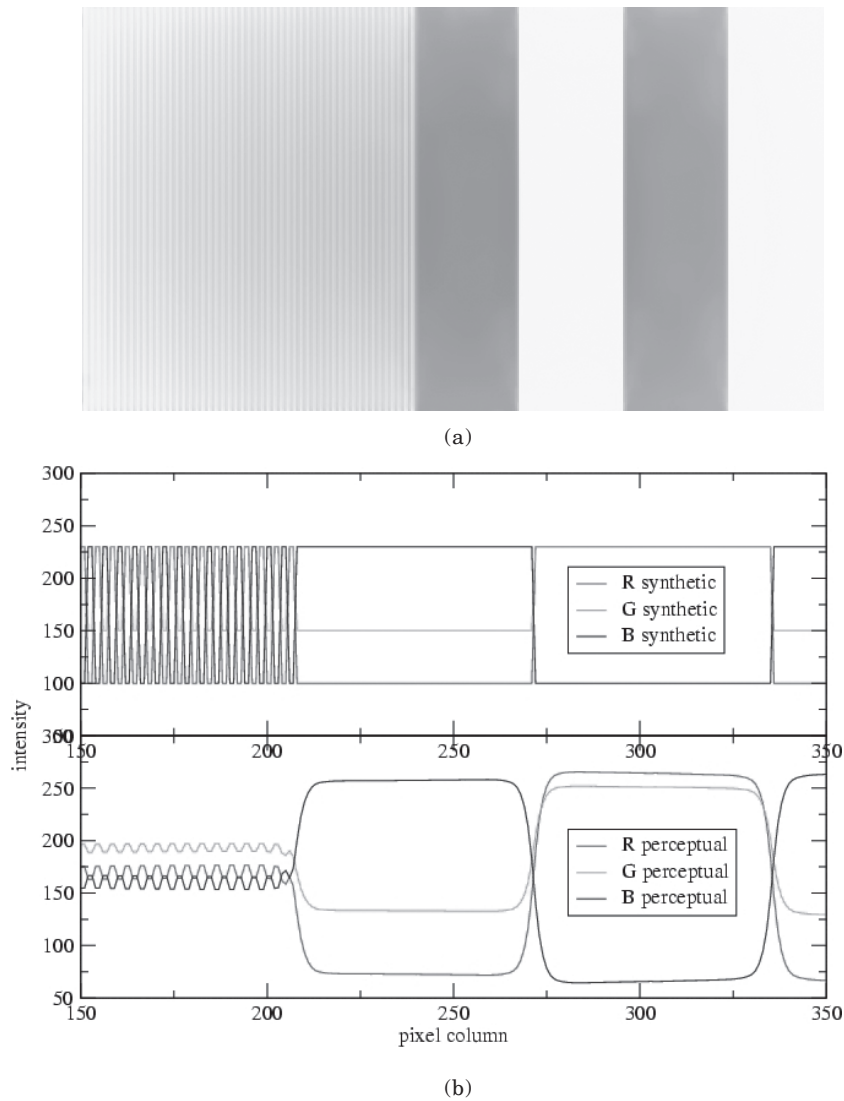
Figure 3. (a) Perceptual image of Fig. 1, taking $j_{thr} = 2$; and (b) profiles of a row from the original image (top) in Fig. 1 and the perceptual image (bottom). *Supplemental Material—Figure 3 can be found in color on the IS&T website (www.imaging.org) for a period of no less than two years from the date of publication.*

of Gaussians) functions in a multiscale framework. The processing of the multiscale decomposition is performed using a linear transformation and a normalization of the filters output. In the present model, processing of the different frequencies is performed in a wavelet space which contains, as a particular case, the use of isotropic DOG functions as frequency filters. Furthermore, the processing of the wavelet decomposition is performed using a nonlinear function which includes saturation effects.

Examples
To evaluate the performance of the proposed model, in this section we show its behavior on two different types of images, synthetic and natural images.

Synthetic Images
One of the synthetic images is shown in Fig. 1, and its perceptual image is shown in Fig. 3. Profiles from a row of these two images are shown in Fig. 3(a). To ease the visualization of this example, the RGB values are shown instead of the opponent values. As shown in these profiles, high frequency features are blurred producing an

almost uniform color, which is shown as a reduction of the radiometric range values. In the low frequency features from the right half of the image, situation is the opposite: wide stripes present a chromatic contrast effect, shown as an increased radiometric distance between them.

A set of synthetic images, shown in Fig. 4, were created to test the behavior of the model. All gratings contain the same number of red, green, blue and yellow bars, but the spatial distribution in every image is different. Particularly, in Figs. 4(a) and 4(b) yellow and red bars are interchanged; in Figs. 4(c) and 4(d) yellow, green, and blue bars are interchanged, but red bars are preserved.

The obtained perceptual images applying the model proposed in Eq. (15), are shown in Fig. 5. Pixels of the perceptual images from Fig. 5 are shown in the 3-dimensional RGB space in Fig. 6. The distribution of the pixels of the original images in RGB space is the same for all of them, because the only difference between the images is the spatial distribution, not their color. Since there are only four colors, i.e., yellow, green, red and blue, we do not show this distribution because it is de-
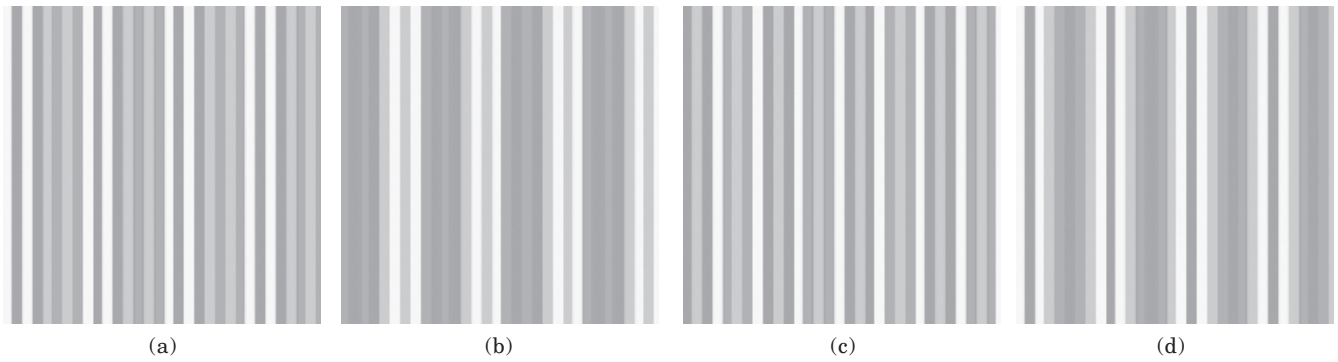
Figure 4. Set of synthetic images. All the images contain the same number of red, green, blue, and yellow bars, but with different spatial distribution. *Supplemental Material—Figure 4 can be found in color on the IS&T website (www.imaging.org) for a period of no less than two years from the date of publication.*
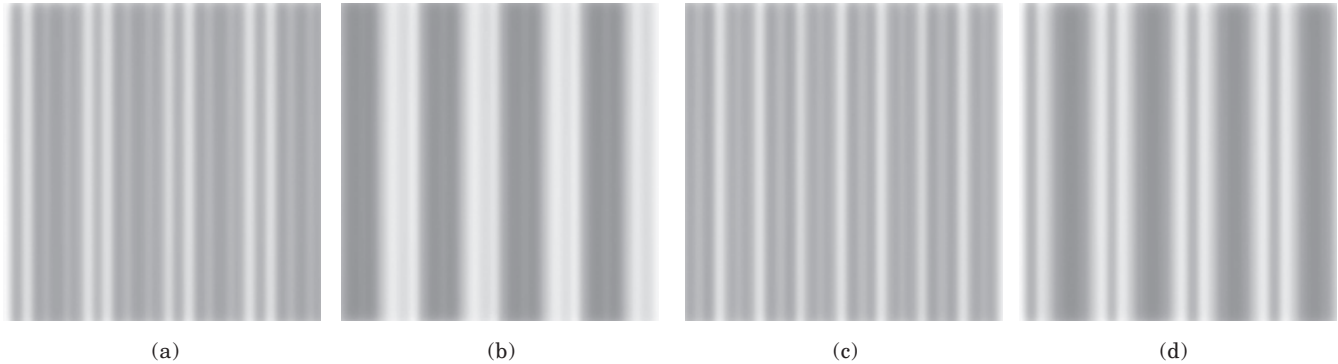
Figure 5. Perceptual images of the corresponding original images in Fig. 4. *Supplemental Material—Figure 5 can be found in color on the IS&T website (www.imaging.org) for a period of no less than two years from the date of publication.*
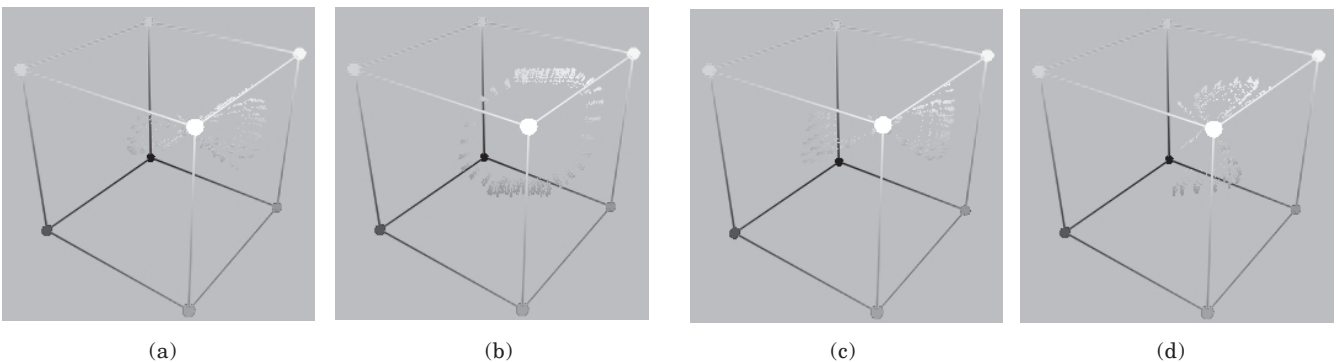
Figure 6. Color representation in the RGB space of the corresponding perceptual images in Fig. 5. *Supplemental Material—Figure 6 can be found in color on the IS&T website (www.imaging.org) for a period of no less than two years from the date of publication.*

fined by just four values in 3-dimensional RGB space, and such a distribution is difficult to see. As expected, the final RGB pixel distributions of the perceptual images are different, because spatial distribution defines the chromatic induction process. Every different spatial distribution of color gratings will produce different final colors, hence it will produce different RGB color distributions. When the patterns are arranged in such a way that global spectral frequency can decrease, then chromatic contrast is applied, and an sparser color distribution is obtained, as is shown in Fig. 6(b).

Natural Scenes
Several images from different natural scenes have also been studied. Since every type of image is used in differ-

ent real situations (art, industry, etc.), different challenges are presented to the method. These images are used to compare the behavior of the usual Gaussian scale-space representation,[3] obtained by applying Gaussian filters to the original image to the wavelet based proposed method. Using a Gaussian scale-space representation, we aim to obtain the perceived images when the original image is observed at increasing distances. At close observation distances, image sharpening should be performed trying to simulate a chromatic contrast effect. At increasing distances, chromatic contrast effect is reduced and chromatic assimilation is increased.

An image from a painting is shown in Fig. 7, its Gaussian scale-space representation is shown in Fig. 8, and the wavelet based perceptual images are shown in

Figure 7. Original image of a painting. *Supplemental Material—Figure 7 can be found in color on the IS&T website (www.imaging.org) for a period of no less than two years from the date of publication.*

Fig. 9. Images from the Gaussian scale-space were obtained using Gaussian filters with increasing standard deviation. Wavelet based images were obtained with increasing values of j_{thr}.

As can be seen, images from the Gaussian scale-space show only the blurring process associated to the chromatic assimilation effect, but wavelet based images are simultaneously blurred and sharpened. For example, the wavelet based perceptual images show enhanced colors and, at the same time, a blurred appearance on the smaller features. A detail of wavelet based and Gaussian based perceptual images is shown in Fig. 10. The wavelet based perceptual image shows redder and more yellow details than the corresponding Gaussian based image, but the same degree of blurring has been applied to small features.

A different situation is presented in the images shown in Fig. 11(a). This is an image taken from a paper printed with a wood grain pattern. Segmentation is required in order to calibrate separately the composition of the inks. In this situation, an image sharpening would produce an image that would be easier to segment. To perform pure image sharpening without image blurring, i.e., chromatic contrast without chromatic assimilation, the wavelet based model simply takes $j_{thr} = 0$, i.e., a close observation distance. The resulting image is shown in Fig. 11(b).

Another different type of image is shown in Fig. 12(a). This textile is made of many different color fibers, and we want to estimate the perceived color in some areas of the image when observing the textile from a certain distance. It implies we want to ignore the color of individual fibers and threads. A wavelet based perceptual image is shown in Fig. 12(b). We can see that colors of individual fibers are similar to that of the surrounding fibers, and at the same time dark grains show an increased contrast compared to surrounding areas. The method allows us to perform color measurement on such a textured image.
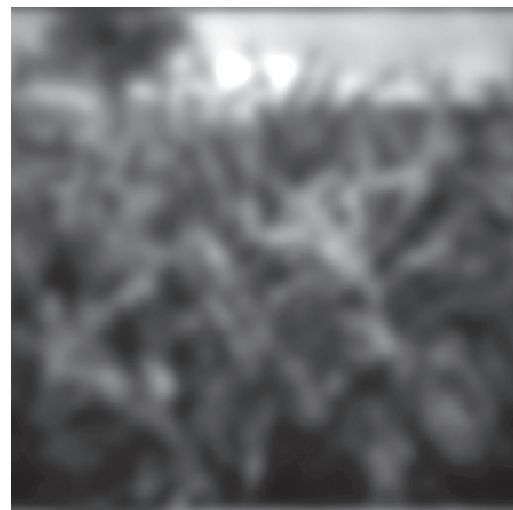
In the example in Fig. 13, fine grains in the stone are blurred but general contrast of wider features are enhanced. In Figs. 14 and 15 we can see some further examples with synthetic images. In Figs. 14(a) and 14(b)
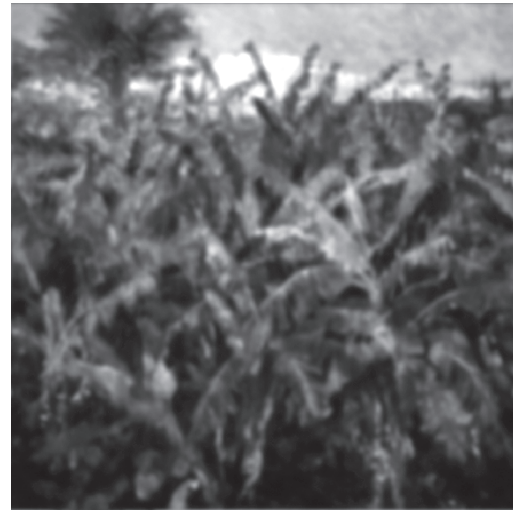

(a)

(b)

(c)

Figure 8. Gaussian scale-space representation of painting image obtained with Gaussian based filters. Observation distance is increased from (a) to (c). Standard deviation of Gaussian kernels are σ = 1.0, 2.0 and 3.0, respectively for every image. *Supplemental Material—Figure 8 can be found in color on the IS&T website (www.imaging.org) for a period of no less than two years from the date of publication.*

(a)
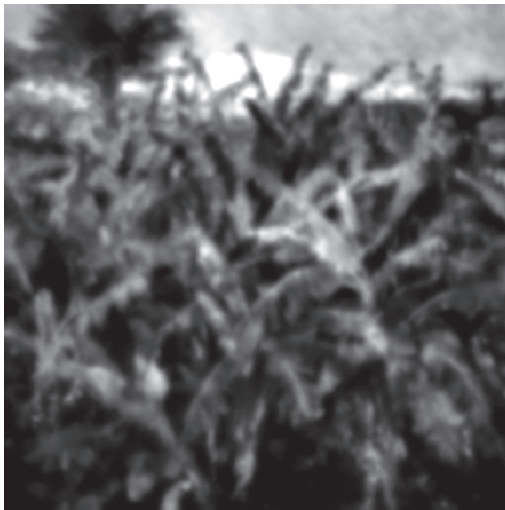
(b)

(c)

**Figure 9.** Perceptual representation of paintings obtained by the wavelet based method. Observation distance is increased from (a) to (c). Induction thresholds used are j_{thr} = 2, 3 and 4, respectively for every image. *Supplemental Material—Figure 9 can be found in color on the IS&T website (www.imaging.org) for a period of no less than two years from the date of publication.*
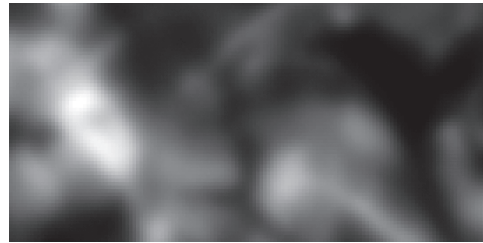
(a)

(b)

Figure 10. (a) Detail of image from the wavelet based perceptual image in Fig. 9(b); and (b) detail of image from the Gaussian scale-space representation in Fig. 8(b). *Supplemental Material—Figure 10 can be found in color on the IS&T website (www.imaging.org) for a period of no less than two years from the date of publication.*
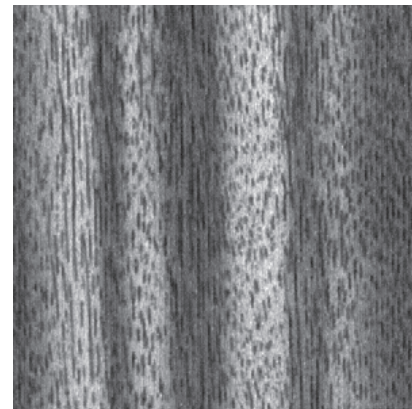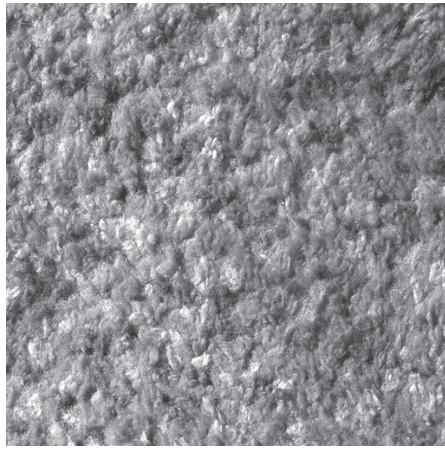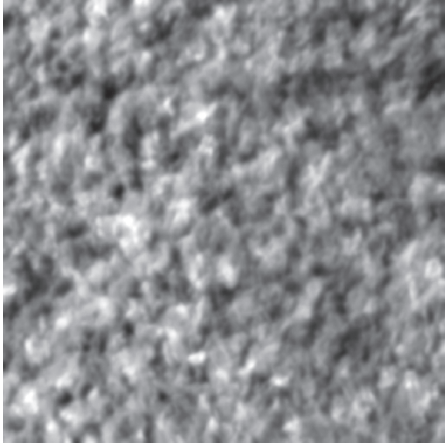

(a)
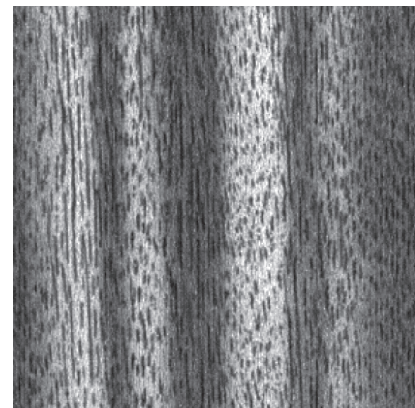
(b)

Figure 11. (a) Original image of simulated wood; and (b) perceptual image obtained with the proposed method when observed at short distance, e.g., j_{thr} = 0. *Supplemental Material—Figure 11 can be found in color on the IS&T website (www.imaging.org) for a period of no less than two years from the date of publication.*

Figure 12. (a) Image of fabric textile; and (b) perceptual image using $j_{thr} = 1$. *Supplemental Material—Figure 12 can be found in color on the IS&T website (www.imaging.org) for a period of no less than two years from the date of publication.*
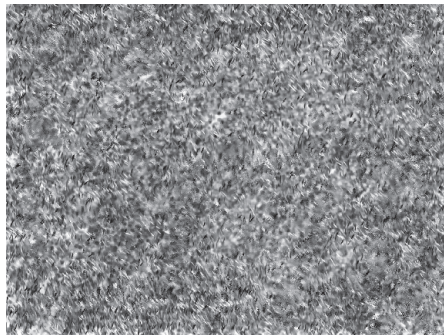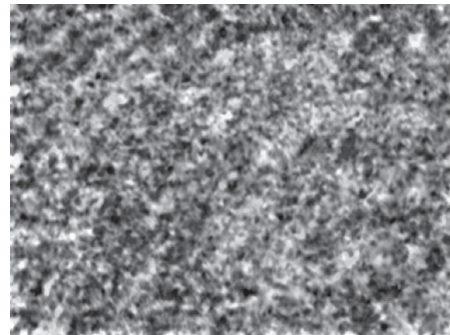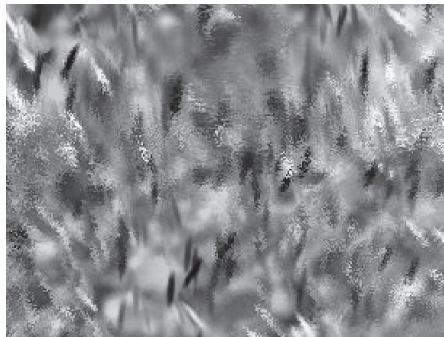

Figure 13. (a) Image of stone; and (b) perceptual image using $j_{thr} = 1$. *Supplemental Material—Figure 13 can be found in color on the IS&T website (www.imaging.org) for a period of no less than two years from the date of publication.*
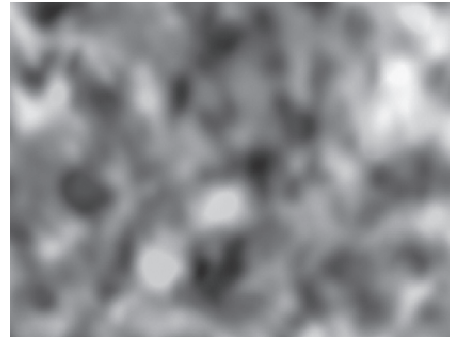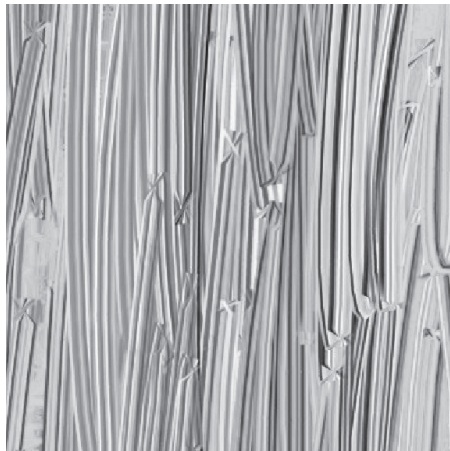

Figure 14. (a) Synthetic image; (b) perceptual image using $j_{thr} = 4$; (c) detail of image (a); and (d) corresponding detail of image (b). *Supplemental Material—Figure 14 can be found in color on the IS&T website (www.imaging.org) for a period of no less than two years from the date of publication.*

(a)

(b)

Figure 15. (a) Synthetic image; and (b) perceptual image using $j_{thr} = 4$. *Supplemental Material—Figure 15 can be found in color on the IS&T website (www.imaging.org) for a period of no less than two years from the date of publication.*

ferent chromatic induction effects. The model presented in this article uses a multiresolution wavelet framework that defines these different chromatic induction effects in a unified mathematical function, and allows us to implement both induction effects using a single perceptual operator. We have shown how the proposed model predicts the expected behavior on synthetic images. We also present some examples of practical applications where building perceived images may allow solution of problems of color measurement on textured images. ▲

References

1. T. Lindeberg, *Scale-Space Theory in Computer Vision*, Kluwer Academics, Dordrecht, The Netherlands, 1994.
2. H. Spitzer and S. Semo, Color constancy: a biological model and its application for still and video images, *Pattern Recognition* **35,** 1645 (2002).
3. M. Vanrell, R. Baldrich, S. Salvatella, R. Benavente, and F. Tous, Induction operators for a computational colour texture representation, *Computer Vision and Image Understanding* **94,** 92 (2004).
4. B. A. Wandell, *Foundations of Vision*, Sinauer Associates Inc., Sunderland, MA, 1995.
5. M. Mirmehdi and M. Petrou, Segmentation of color textures, *IEEE Trans. Pattern Anal. Machine Intell.* **22,** 142 (2000).
6. G. Wyszecki, Color Appearance, in *Handbook of Perception and Human Performance*, L. K. K. R. Boff and J. P. Thomas, Eds., Sensory Processes and Perception series, vol. 1, John Wiley, London, 1986.
7. V. C. Smith, P. Q. Jin and J. Pokorny, The role of spatial frequency in color induction, *Vision Res.* **41,** 1007 (2001).
8. E. H. Land, The retinex theory of color vision. *Scientific Amer.* 108 (1997).
9. R. Shapley and C. Enroth-Cugell, Visual adaptation and retinal gain control, *Rev. Psychol.* **41,** 635 (1984).
10. G. Westheimer, Center-surround antagonism in spatial vision: Retinal or cortical locus?, *Vision Res.* **44,** 2457 (2004).
11. S. Mallat, *A Wavelet Tour of Signal Processing*, 2nd ed., Academic Press, San Diego, CA, 1999.
12. C. K. Chui, *An Introduction to Wavelets*, Academic Press, Boston, MA, 1992.
13. I. Daubechies, *Ten Lectures on Wavelets*, SIAM Press, Philadelphia, PA, 1992.
14. M. Holschneider and P. Tchamitchian, *Les ondelettes en 1989*, P.G. Lemari, Ed., Springer-Verlag, Paris, France, 1990.
15. P. J. Burt and E. H. Adelson, The Laplacian pyramid as a compact image code, *IEEE Trans. Commun.* **COM-31,** 532 (1983).
16. E. Brenner, J. S. Ruiz, E. M. Herraiz, F. W. Cornelissen, and J. B. J. Smeets, Chromatic induction and the layout of colours within a complex scene, *Vision Res.* **43,** 1413 (2003).
17. A. Werner, The spatial tunning of chromatic adaptation, *Vision Res.* **43,** 1611 (2003).
18. A. Poirson and B. Wandell, The appearance of colored patterns: Pattern-color separability, *J. Opt. Soc. Amer. A*, **10,** 2458 (1993).
19. A. B. Poirson and B. A. Wandell, Pattern-color separable pathways predict sensitivity to simple colored patterns, *Vision Res.* **36,** 515 (1996).
20. B. Blakeslee and M. E. McCourt, A Multiscale spatial filtering account of the White effect, simultaneous brightness contrast and grating induction, *Vision Res.* **39,** 4361 (1999).
21. B. Blakeslee and M. E. McCourt, A unified theory of brightness, contrast and assimilation incorporating oriented multiscale spatial filtering and contrast normalization, *Vision Res.* **44,** 2483 (2004).

we can see original and perceptual images. In Figs. 14(c) and 14(d) we show some details from them. We can see that the most noisy areas are completely blurred, and, in the Supplemental Material, that some new colors appear as a consequence of the assimilation process between some color features. Wider features show greater contrast with respect to the surrounding areas. The same behavior is observed in Figs. 15(a) and 15(b).

Conclusions
Features at different spatial scale or resolution, i.e., features with different frequency information, induce dif-